Journal of Inclusion Phenomena and Macrocyclic Chemistry **41:** 163–172, 2001.

Complexation of Porphyrin-Appended Guests by Calix[4]arene-Appended Cyclodextrins

JASPER J. MICHELS, ROBERTO FIAMMENGO, PETER TIMMERMAN, JURRIAAN HUSKENS* and DAVID N. REINHOUDT*

Laboratory of Supramolecular Chemistry and Technology, MESA$^+$ Research Institute, University of Twente, P.O. Box 217, 7500 AE Enschede, The Netherlands (Phone: +31 53 4892980, Fax: +31 53 4894645, E-mail: smct@ct.utwente.nl)

(Received: 15 July 2001; in final form: 31 August 2001)

Key words: cyclodextrins, porphyrins, calix[4]arenes, microcalorimetry

Abstract

A calix[4]arene based β-cyclodextrin dimer and tetramer (**1** and **2**, Figure 1) were synthesized by covalent attachment of a mono(2-*O*-xylylamino)-β-cyclodextrin derivative to calix[4]arene platforms, bi- or tetrafunctionalized with carboxylic acid groups at their upper rims. The complexation of porphyrin-based guest molecules by these hosts in water was studied using microcalorimetry. Tetrakis(4-phenylsulfonato)porphyrin (TsPP) binds to **2** in a 1 : 2 (host : guest) fashion with enhanced binding strength ($K_1 = 6.6 \times 10^6$ M^{-1}) as compared to the monomeric TsPP–CD interaction ($K = 8.8 \times 10^5$ M^{-1}). This enhancement is attributed to the involvement of two cyclodextrin units in the accommodation of one TsPP guest. Increase of the number of 4-sulfonatophenyl sites on the guest by generating the μ-oxo-dimer of the iron(III) complex of TsPP led to further increase of the binding strength owing to participation of three β-cyclodextrin cavities of **2** ($K = 1.5 \times 10^7$ M^{-1}). The geometric incompatibility between host and guest, stemming from the fact that both TsPP and its μ-oxo-dimer are fairly small compared to the multi-cyclodextrin hosts, probably explains why the enhancement is still moderate. A much more pronounced increase in complexation strength was achieved with *p*- and *m*-pyridylporphyrin extended with *p-tert*-butylbenzyl guest sites. These guests are large enough to accommodate three to four β-cyclodextrin units. The better match in size between host and guest gave association constants up 10^8 and 10^9 M^{-1} for the β-cyclodextrin dimer and tetramer, respectively. In fact, the 1 : 1 complex between tetrakis*(p-tert*-butylbenzyl)-*p*-pyridylporphyrin and **2** ($K = 5 \times 10^9$ M^{-1}) is the strongest reported for cyclodextrin–porphyrin interactions.

Introduction

Porphyrins play an important catalytic role in many biological processes such as photosynthesis and oxygen transfer in organic tissues [1]. Generally, porphyrins have a relatively large hydrophobic surface area and hence exhibit low intrinsic solubility in water. In nature, the porphyrin unit is accommodated into a hydrophobic region of a protein, the hydrophilic groups present in the peripheral region providing water solubility to the conjugate. Another advantage is that encapsulation of the porphyrin by the protein prevents dimerization into catalytically inactive μ-oxo-porphyrin dimers. Examples of such systems are heme proteins (hemoglobin and myoglobin). Heme proteins have been modeled extensively by synthetically obtained capped and fenced porphyrins [2]. More recently, a catalytically active porphyrin was equipped with four α-helical polypeptide chains upon self-assembly in water [3].

Cyclodextrins templated on a molecular platform may as well accommodate catalytically active porphyrins in aqueous solution by complexation of hydrophobic binding sites (e.g. phenyl groups) of the porphyrins into the cyclodextrin cavities. For this reason, the non-covalent interactions between porphyrins and native α-, β-, and γ-cyclodextrins [4, 5], partly- [6] or per-methylated β-cyclodextrin [7, 8], β-cyclodextrin dimers [9–11] or a β-cyclodextrin tetramer [12] in water have been studied extensively. The strongest association constants were found for β-cyclodextrin dimers: generally in the order of 10^5–10^6 M^{-1}. If the porphyrins are metallated and the spacing unit of the cyclodextrin dimer contains an apically ligating group, the binding strength may be enhanced to about 10^7–10^8 M^{-1}, owing to complexation of the metal center to the spacer.

Here we report the synthesis and guest-binding properties of calix[4]arene-templated β-cyclodextrin dimer **1** and tetramer **2** in water (Figure 1). In view of the size and symmetry of **1** and **2**, porphyrin-appended guests are anticipated to be appropriate guest molecules for the formation of strong complexes in water. The cooperativity of the cyclodextrins in binding of the porphyrins is investigated as well as the effect of structural variations of the porphyrin guests on binding strength and cooperativity. The studies include guests based on tetrakis(4-sulfonatophenyl)porphyrin (TsPP) as well as pyridylporphyrins. The binding of the latter by multi-

* Authors for correspondence.

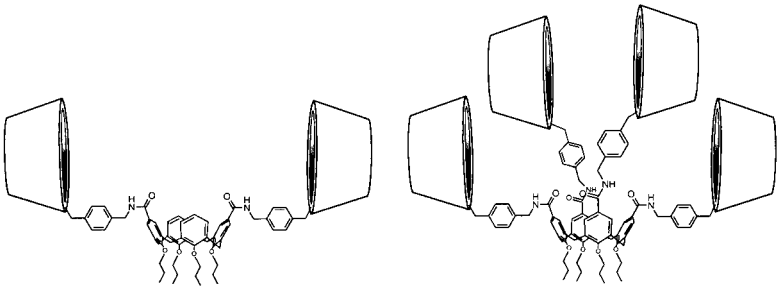

1 2

Figure 1. Calix[4]arene-based β-cyclodextrin dimer **1** and tetramer **2**.

cyclodextrin hosts is described for the first time and reveals the formation of the strongest cyclodextrin–porphyrin complex reported to date. Most of the studies described in this chapter were carried out using isothermal titration microcalorimetry. Trends in thermodynamic parameters (ΔG^0, ΔH^0, and $T\Delta S^0$) upon complexation of porphyrin-based guests by cyclodextrin-based hosts in water provide essential information on complex stability, stoichiometry, and geometrical constraints.

Experimental

Tetrapropoxycalix[4]arene dicarboxylic acid **3** [13], tetrapropoxycalix[4]arene tetracarboxylic acid **4** [13], β-cyclodextrin building block **5** [14], and heptakis(2-*O*-methyl)-β-cyclodextrin **6** [14] were synthesized according to literature procedures.

*Calix[4]arene-based β-CD dimer **1***

Tetrapropoxycalix[4]arene dicarboxylic acid **3** (14 mg, 0.021 mmol) was stirred overnight in an excess of $SOCl_2$ at 80 °C. Accordingly, the excess of thionyl chloride was removed by evaporation under vacuum. To the remaining white solid CH_2Cl_2 was added as a solvent. Subsequently, a mixture of TBDMS-protected β-cyclodextrin building block **5** (97 mg, 0.045 mmol) and Et_3N (50 μL, 0.36 mmol, d = 0.728 g mL^{-1}) in CH_2Cl_2 was added dropwise at room temperature. The solution was stirred for 15 min at room temperature. Subsequently, the reaction mixture was washed twice with 0.1 M HCl(aq) and once with water. The organic layer was dried over Na_2CO_3. The product was purified over silicagel using CH_2Cl_2 : MeOH = 30 : 1 as the eluent (R_f = 0.4) and used as such in the deprotection step without characterization. TBDMS-protected β-cyclodextrin precursor of **1** (90 mg, 0.018 mmol) was dissolved in THF at room temperature. Accordingly, 366μL (0.36 mmol) of a 1 M solution of tetrabutylammonium fluoride (TBAF) in THF was added to the solution. The reaction mixture was refluxed (66 °C) over night. Accordingly, the solvent was evaporated *in vacuo* and the residue was diluted with water. The aqueous layer was washed twice with diethyl ether. The excess of TBAF was removed by eluting the product several times over an amberlite MB3 mixed H^+/OH^- ion exchange column. Calix[4]arene-based β-cyclodextrin dimer **1** was obtained as a white solid in 47 mg (71% overall). ^{1}H-NMR (CD_3OD) δ 7.62–7.40 (br m, 10H, ArH), 6.37–6.12 (m, 8H, ArH), 5.06–3.25 (m, 188H), 1.92 (m, 8H, calix CH_2CH_3), 1.12 (m, 6H, calix CH_3), 0.93 (m, 6H, calix CH_3); ^{13}C-NMR (CD_3OD) δ 168.2, 154.6, 153.4, 135.5, 134.2, 128.0, 127.5, 126.8, 101.2, 99.9, 83.1, 81.5, 78.2, 76.2, 72.4, 72.0, 71.6, 71.1, 59.8, 58.5, 57.9, 42.4, 29.9, 22.6, 22.4, 9.4, 8.5; MALDI-TOF-MS Calcd. for $C_{154}H_{226}O_{76}N_2$: *m/z* = 3319.4, Found: *m/z* = 3367.7 ($[M–H + 2Na]^+$).

*Calix[4]arene-based β-cyclodextrin tetramer **2***

Calix[4]arene-based β-cyclodextrin tetramer **2** was synthesized following a procedure analogous to the synthesis of β-cyclodextrin dimer **1** starting with 20 mg (0.026 mmol) of tetrapropoxycalix[4]arenetetracarboxylic acid **4** and 228 mg (0.11 mmol) of TBDMS-protected β-cyclodextrin building block **5**. After deprotection, product **2** was obtained in 79 mg (76% overall). ^{1}H-NMR (DMSO) δ 8.49 (br, 4H), 7.36–7.26 (m, 24H), 5.2–3.0 (br m, 354H), 1.91 (br, 8H), 0.98 (t, 12H, J = 6.8 Hz, calix CH_3); ^{13}C-NMR (DMSO) δ 165.8, 158.5, 134.0, 128.3, 128.0, 127.7, 127.2, 101.0, 99.6, 81.8, 72.7, 72.3, 71.5, 59.9, 59.5, 59.4, 59.0, 38.4, 22.7, 10.1; MALDI-TOF-MS Calcd. for $C_{268}H_{402}O_{148}N_4$: *m/z* = 6044.5, Found: *m/z* = 6066.4 ($[M + Na]^+$).

*HPLC analysis of **1** and **2***

Since no satisfactory elemental analysis could be obtained for **1** and **2**, their purity was proven using a Waters 600 Controller HPLC coupled to a Waters 996 diode array detector in combination with a μBondapak C_{18} 125 Å 10 μm column (size: 3.9 × 300 mm). Eluent: acetonitrile/water 70 : 30 (v/v) and 60 : 40 (v/v) for **1** and **2**, respectively.

*Tetrakis(p-tert-butylbenzyl-p-pyridyl)porphyrin **10** tetrachloride salt*

Analogous to a literature procedure [15], a solution of 5,10,15,20-tetra(*p*-pyridyl)porphyrin and α-bromo-*p*-*tert*-butyltoluene in DMF was stirred for 8–12 h at 80 °C. After removal of DMF, the solids were triturated with ether and dissolved in methanol. A solution of NH_4PF_6 in water was added upon which a precipitate formed. The precipitate was filtered off and washed with water and ether. The water-soluble chloride salt of the product was obtained by subjecting the PF_6 salt to an anion exchange column (DOWEX

1-X8, 50–100 mesh, Cl-form) using acetonitrile/water (1/1 v/v) as the eluent. ^{1}H-NMR (CD_3OD) δ 9.49 (d, 8H, J = 6.4 Hz), 9.15 (bs, 8H), 8.97 (d, 8H, J = 6.4 Hz), 7.74 (m, 16H), 6.19 (s, 8H), 1.40 (s, 36H); ^{13}C-NMR (CD_3OD) δ 159.9, 155.0, 144.5, 134.5, 131.4, 130.7, 128.0, 117.0, 65.8, 35.8, 31.7; IR (KBr) 3422, 3114, 3031, 2962, 2868, 1636, 1508, 1458, 1155, 847, 796; UV-vis (MeOH) 650, 592, 554, 517, 427; Anal. Calcd. for $C_{84}H_{86}N_8Cl_4 \cdot 9.4H_2O$: C, 66.43; H, 6.95; N, 7.38, Found: C, 66.42; H, 6.58; N, 7.27.

*Tetrakis(p-tert-butylbenzyl-m-pyridyl)porphyrin **11** tetrachloride salt*

Tetrakis(*p-tert*-butylbenzyl-*m*-pyridyl)porphyrin **11** tetrachloride salt was synthesized following a procedure analogous to the synthesis of **10** using 5,10,15,20-tetra(*m*-pyridyl)porphyrin as the starting compound. ^{1}H-NMR (CD_3OD) δ 10.10 (m, 4H), 9.58 (d, 4H, J = 6.0 Hz), 9.44 (d, 4H, J = 7.9 Hz), 8.61 (m, 4H), 7.65 (m, 16H), 6.18 (s, 8H), 1.34 (s, 36H); ^{13}C-NMR (CD_3OD) δ 154.9, 150.4, 148.3, 145.8, 143.8, 143.2, 131.7, 130.8, 128.5, 127.9, 114.4, 66.2, 35.7, 31.6; IR (KBr) 3414, 3068, 2962, 2868, 1628, 1499, 1465, 1196, 979, 794; UV-vis (MeOH) 643, 586, 544, 512, 422; Anal. Calcd. for $C_{84}H_{86}N_8Cl_4 \cdot 8.9H_2O$: C, 66.82; H, 6.93; N, 7.42, Found: C, 66.85; H, 6.57; N, 7.30.

Measurements

All titrations were carried out in doubly distilled water (Q2) at 25 °C, unless mentioned otherwise.

Calorimetric titrations

Calorimetric measurements were carried out using a Microcal VP-ITC microcalorimeter with a cell volume of 1.4115 mL. The titrant typically contained 0.1–10 mM of host or guest while the cell solutions had 10–600 μM of guest or host. Calorimetric dilution expriments showed that at the experimental concentrations none of the porphyrin-based guests showed significant aggregation behavior. The same holds for the calix[4]arene-based hosts **1** and **2**. Titrations involving Fe^{III}TsPP **8** (at pH 3) and μ-oxo-porphyrin dimer **9** (at pH 10) were carried out in the presence of 0.1 M NaCl as a background electrolyte in order to establish the same ionic strength as in the UV-vis titrations. The pH was adjusted using 1 M HCl and 1 M NaOH, respectively. Dilution experiments proved that **8** and **9** do not aggregate in the presence of 0.1 M NaCl at the experimental concentrations. All other titrations were carried out in the absence of a background electrolyte in order to avoid interfering aggregation processes of the porphyrin-based guests.

UV-vis titrations

UV-vis measurements were carried out using a Hewlett Packard 8452A diode array spectrophotometer. Stock solutions were prepared containing 10.0 μM of Fe^{III}TsPP (**8**), 10 mM KH_2PO_4, and 90 mM NaCl (I = 0.1). One of the stock solutions also contained 10.0 μM of **2**. Accordingly, 8–10 samples were taken from the solutions and their pH was adjusted using 1 M NaOH or HCl. The small changes in concentration upon adjusting the pH were neglected. Subsequently, separate UV-vis spectra were recorded using the samples.

^{1}H NMR titrations

NMR spectra were recorded using a Varian Inova 300 NMR spectrometer. ^{1}H NMR chemical shifts (300 MHz) are given relative to residual CHD_2OD (3.30 ppm), h,d_5-DMSO (2.50 ppm), or HDO (4.65 ppm) unless mentioned otherwise. ^{13}C chemical shifts (75 MHz) are given relative to CD_3OD (49.0 ppm), or d_6-DMSO (39.5 ppm) unless mentioned otherwise. Pyridylporphyrins **10** and **11** (guests) were titrated with β-cyclodextrin (host), monitoring the chemical shift of the porphyrin protons upon interaction with the host. For the titrations of **10** and **11** with β-cyclodextrin stock solutions were prepared containing 0.5 mM and 2.0 mM of the guest and the host, respectively. Subsequently, ^{1}H NMR spectra were recorded of mixtures of varying amounts of the guest and host stock solution, maintaining a total volume of 0.8 mL in each sample. The end points of both titrations represent a situation in which the host is present in 27 fold excess relative to the guest.

Results and discussion

The lower rim of calix[4]arene was alkylated using *n*-iodopropane, yielding the platform in its cone conformation. For **2** the calix[4]arene lower rim was tetraalkylated in one step using NaH to deprotonate the lower rim OH-groups. Subsequent tetrafunctionalization of the upper rim with Br functionalities was achieved via reaction of the tetraalkylated calix[4]arene with *N*-bromosuccinimide (NBS) [16]. For **1**, selective dialkylation at the calix[4]arene 25- and 27-positions was carried out using K_2CO_3 as a base [17]. Reaction of the dialkylated species with bromine resulted in selective introduction of Br functionalities at the non-alkylated phenol rings of the calix[4]arene, since these positions are activated towards electrophilic aromatic substitution by the phenolic *para*-OH-groups at the calix[4]arene lower rim [18]. The remaining free positions at the lower rim were alkylated using *n*-iodopropane and NaH. Lithiation of the di- or tetrabromocalix[4]arenes and subsequent reaction of the di- and tetralithiates with *N*,*N*-dimethylformamide (DMF) yielded the corresponding aldehydes [13]. Finally, oxidation of the aldehydes gave calix[4]arene carboxylic acid building blocks **3** and **4** (see Scheme 1) in high yields [19].

The β-cyclodextrin building block **5** involved protection of β-cyclodextrin at the primary side with TBDMS groups, monofunctionalization of the secondary side at a C2-OH position with a xylyl-spaced cyano moiety, and methylation of the remaining C2-OH groups as described before [14]. Reduction of the cyano group yielded the primary amino-appended β-cyclodextrin **5**.

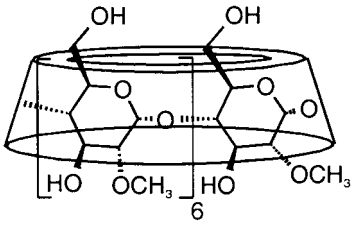

6

Figure 2. Heptakis(2-O-methyl)-β-cyclodextrin **6**.

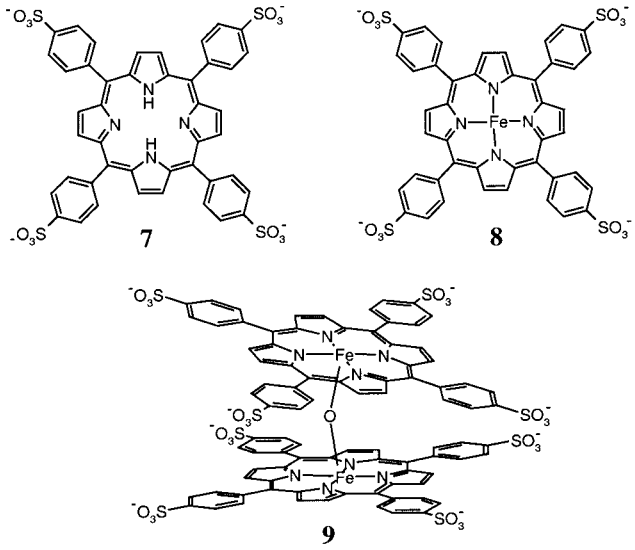

Figure 3. TsPP-based porphyrin guests (counterions and iron-coordinated water molecules are omitted).

Scheme 1 shows the synthesis of β-cyclodextrin dimer **1** and tetramer **2** by linking **5** to calix[4]arenes **3** and **4** via an amide coupling reaction with the formation of the TBDMS-protected precursors of **1** and **2**. This reaction involved conversion of **3** and **4** into the corresponding acid chlorides, which were reacted with **5** without purification. Subsequent deprotection using tetrabutylammonium fluoride (TBAF) in THF yielded the water-soluble products **1** and **2**.

Heptakis(2-*O*-methyl)-β-cyclodextrin **6** (Figure 2) was synthesized as a reference compound by reaction of primary side TBDMS-protected β-cyclodextrin with dimethylsulfate under basic conditions [14]. Subsequent deprotection using TBAF in THF yielded the water-soluble host **6**.

A water-soluble porphyrin of which the interaction with cyclodextrin monomers [4, 5, 7, 20], and dimers [10, 11] in water has been previously studied by spectroscopic techniques, is tetrakis(4-sulfonato)-tetraphenylporphyrin (TsPP **7**, Figure 3). Four binding sites for cyclodextrin, the 4-sulfonatophenyl moieties, are attached to the aromatic porphyrin ring, which functions as a flat and rigid platform, too large to be included into a β-cyclodextrin cavity. For the present study TsPP **7**, its iron(III) complex **8**, and μ-oxo-dimer **9** [21] were selected as guests for binding to β-cyclodextrin dimer **1** and tetramer **2**.

Although previously it has been assumed that four β-cyclodextrins can complex to TsPP **7** [20] more recent studies proved that native β-cyclodextrin binds to **7** in a 2 : 1 fashion, complexing two opposite 4-sulfonatophenyl groups [5]. Complexation of two adjacent binding sites is sterically less favorable and gives rise to weaker complexation [9]. The binding in water of TsPP **7** to β-cyclodextrin dimer **1** or tetramer **2** was studied with isothermal titration microcalorimetry. In Figure 4 the net heat evolved per injection is plotted against the molar ratio of guest and host. The host : guest stoichiometries for the complexes of **1** and **2** with **7** are 1 : 1 and 1 : 2, respectively, expressed by the inflection points of the binding isotherms. These stoichiometries suggest that two cyclodextrin cavities are involved in the binding of TsPP, in agreement with the studies mentioned above.

The data obtained from the titration of β-cyclodextrin dimer **1** with TsPP **7** were fitted to a 1 : 1 binding model using the association constant K and the binding enthalpy ΔH^0 as independent fitting parameters. The data obtained from the titration of β-cyclodextrin tetramer **2** with **7** were fitted to a 1 : 2 (host : guest) binding model in which the four binding sites provided by **2** are treated as independent sites. The enthalpies ΔH_1^0 and ΔH_2^0 for the subsequent complexation steps are thus considered equal. Furthermore, it was assumed that TsPP **7** only binds to two adjacent β-cyclodextrin sites of **2** and not to opposite cavities. CPK modeling indicated that a 1 : 2 complex cannot be formed if the first guest binds to two opposite cyclodextrins. All remaining binding possibilities were considered to be degenerate. These assumptions lead to: $K_1 = 8K_2$. Consequently, only K_1 and ΔH_1^0 were varied as independent parameters.

Table 1 shows the resulting values for the parameters K and ΔH^0 after curve fitting of the complexation data of **1** and **2** with **7** as well as the corresponding values for ΔG^0 and $T\Delta S^0$. All parameters are given for the stepwise equilibria. Table 1 also includes the data of a reference titration of heptakis(2-*O*-methyl)-β-cyclodextrin (**6**) to TsPP **7**. Comparison of the binding stoichiometries and enthalpies for the complexation of dimeric β-cyclodextrin host **1** and monomeric β-cyclodextrin host **6** to **7** shows that both β-cyclodextrin cavities of **1** are involved in binding. However, the complex stability for **1** is not enhanced compared to **6**. It was therefore concluded that despite the effective enthalpic contribution of the two sites of β-cyclodextrin dimer **1**, entropic factors probably prohibit effective cooperativity and enhancement of complex stability. An explanation might be that the β-cyclodextrin sites of **1** are spaced too far apart for strong cooperativity.

Also for the complexation of β-cyclodextrin tetramer **2** to TsPP **7** two β-cyclodextrins per TsPP are involved in binding, as indicated by the comparison of complex stoichiometry and binding enthalpy with the values obtained for heptakis(2-*O*-methyl)-β-cyclodextrin **6**. In this case, the enhancement in complex stability is only raised because within one host the four templated β-cyclodextrin sites provide multiple pairs of cyclodextrins that act as complexation site for **7**.

The results described above indicate that, despite the correct number of binding sites, TsPP **7** is too small for

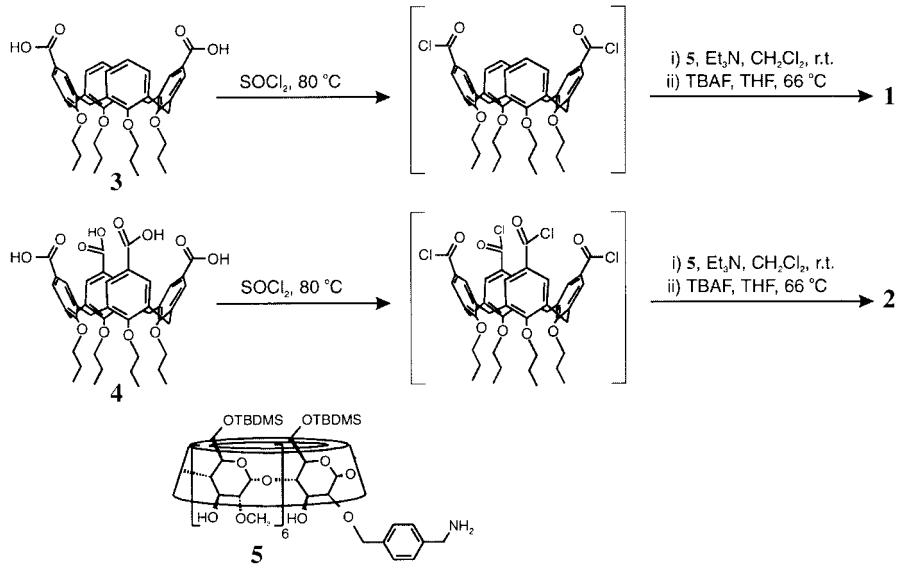

Scheme 1.

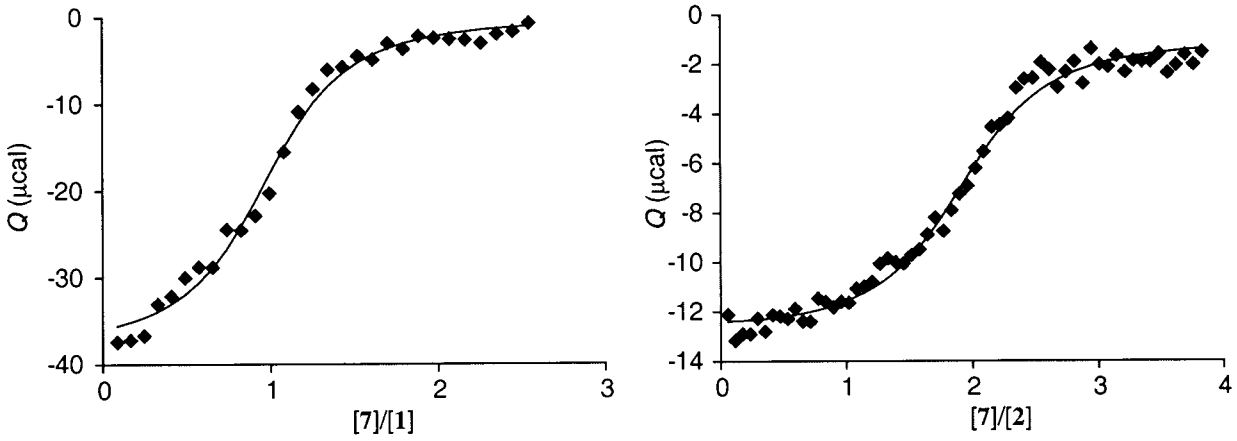

Figure 4. Heat evolved per injection as a function of the ratios [**7**]/[**1**] (left) and [**7**]/[**2**] (right) as observed for the microcalorimetric titrations of TsPP **7** to β-cyclodextrin dimer **1** and β-cyclodextrin tetramer **2**. Lines: fit to a 1 : 1 binding model (left) and a 1 : 2 binding model (right).

binding to more than two β-cyclodextrin sites of tetramer **2**. For this reason, the larger μ-oxo-dimer **9**, having eight 4-phenylsulfonato sites, may be better suited as a guest for β-cyclodextrin tetramer **2**.

The stabilities and stoichiometries of the complexes of μ-oxo-dimer **9** or Fe^{III}TsPP **8** with β-cyclodextrin tetramer **2** in water were determined using microcalorimetry. Fe^{III}TsPP **8** was titrated to **2** at a pH (3), where no μ-oxo-dimer formation occurs according to UV-vis spectroscopy [21]. μ-Oxo-dimer **9** was titrated to **2** at a pH (10), where all porphyrin is dimerized at the concentrations employed here. The complex stoichiometries were found to be 1 : 2 and 1 : 1 (host : guest) for the binding of **8** and **9** to **2**, respectively (Figure 5). Furthermore, when β-cyclodextrin tetramer **2** was titrated to μ-oxo-dimer **9**, a 1 : 2 complex appeared to form at low **2** : **9** ratios. In Table 1, the association constants and thermodynamic parameters obtained from least squares fitting of these titrations are listed. For the complexation of Fe^{III}TsPP **8** to **2**, the binding sites were treated as equivalent ($K_1 = 8K_2$ and $\Delta H_1^0 = \Delta H_2^0$).

The stability constants found for the complexes of **8** to **2** are lower than those found for TsPP **7**. This may be explained by a higher overall polarity of Fe^{III} complex **8**, as compared to **7**. The data obtained from the titrations of μ-oxo-dimer **9** to β-cyclodextrin tetramer **2** and **2** to **9** were fitted simultaneously to a 1 : 2 binding model. The presence of the 1 : 2 complex does, however, not influence the fit of the former (Figure 5, right) significantly.

The relatively high complex stability, the (mainly) 1 : 1 binding stoichiometry, and the large favorable enthalpy change accompanying the complexation of μ-oxo-dimer **9** by β-cyclodextrin tetramer **2** are indicative of the involvement of multiple β-cyclodextrins in strong binding. Moreover, compared to the binding enthalpies found for the monomeric interaction of heptakis(2-*O*-methyl)-β-cyclodextrin **6** to TsPP **7** ($\Delta H^0 = -5.8$ kcal/mol) and the dimeric interaction of Fe^{III}TsPP **8** to β-cyclodextrin tetramer **2** ($\Delta H^0 = -14.3$ kcal/mol) the binding enthalpy for the **2**·**9** complex (−21.4 kcal/mol) roughly suggests that three of the four β-cyclodextrins of **2** bind to μ-oxo-dimer **9** in the 1 : 1 complex. Modeling studies illustrated that the porphyrin

Table 1. Thermodynamic parameters of the complexation of TsPP- and pyridylporphyrin-based guests by β-cyclodextrin dimer **1**, β-cyclodextrin tetramer **2**, heptakis(2-*O*-methyl)-β-cyclodextrin **6**, and β-cyclodextrin as determined by microcalorimetry

Host	Guest	Stoichiometry	K [a]	ΔG^{0} [b]	ΔH^{0} [b]	$T\Delta S^{0}$ [b]
1	**7**	1 : 1	5.9×10^5	−7.9	−12.7	−4.8
	10	1 : 1	$(0.2–2) \times 10^8$	−9.7 to −11.3	−4.1	5.5–7.3
		2 : 1	4.0×10^6	−8.8	−2.7	6.1
	11	1 : 1	2.2×10^6	−8.5	−6.2	0.5
		2 : 1	1.8×10^5	−7.0	−6.1	1.0
2	**7**	1 : 1	6.6×10^6	−9.3	−14.1	−4.8
		1 : 2	8.2×10^5	−8.1	−14.1	−6.1
	8	1 : 1	1.4×10^6	−8.4	−14.3	−5.9
		1 : 2	1.7×10^5	−7.1	−14.3	−7.2
	9	1 : 1	1.5×10^7	−9.9	−21.4	−11.6
		1 : 2	4.2×10^5	−7.7	−4.6	3.1
	10	1 : 1	5×10^9	−12.9	−7.8	5.1
		2 : 1	5×10^6	−8.9	−0.9	8.0
6	**7**	1 : 1	8.8×10^5	−8.1	−5.8	2.3
		2 : 1	1.1×10^5	−6.9	−5.8	1.1
	10	∼4 : 1	$K_1 = 8.6 \times 10^3$		$\Delta H_1^0 = -2.5$	
					$\Delta H_3^0 = -0.8$	
	11	∼4 : 1	$K_1 = 1.6 \times 10^4$		$\Delta H_1^0 = -3.9$	
					$\Delta H_3^0 = 1.1$ [c]	
β-CD	**10**	∼4 : 1	$K_1 = 3.5 \times 10^4$		$\Delta H_1^0 = -4.6$	
					$\Delta H_3^0 = -2.7$	
	11	∼4 : 1	$K_1 = 2.5 \times 10^4$		$\Delta H_1^0 = -6.0$	
					$\Delta H_3^0 = -2.2$	

[a] In M^{-1}.
[b] In kcal/mol^{-1}.
[c] ΔH_3^0 and ΔH_4^0 independently varied.

platforms of **9** are too close together to create enough space to accommodate all four cyclodextrins.

As mentioned above, at high **2** : **9** ratios a **2**·$\mathbf{9}_2$ complex forms. The relatively low value for ΔH_2^0 (−4.6 kcal/mol) indicates the involvement of the fourth cyclodextrin in the **2**·$\mathbf{9}_2$ complex. Most likely, both μ-oxo-dimers **9** are each complexed by two cyclodextrins, implying that one cyclodextrin is decomplexed from the one μ-oxo-dimer **9** in the 1 : 1 complex upon formation of the 1 : 2 complex. This results in a less negative value for ΔH_2^0.

Previous studies have shown that native β-cyclodextrin [20] as well as β-cyclodextrin dimers [22] may hinder μ-oxo-dimer formation because the bulkiness of the complexed macrocycles prevent the porphyrins from approaching each other. The apparent dimerization pH of Fe^{III}TsPP **8** is then shifted to a higher value. In order to find out whether this is true for β-cyclodextrin tetramer **2**, a pH titration involving Fe^{III}TsPP **8** was performed both in the absence and in the presence of tetramer **2** while monitoring the shift of the porphyrin Soret band with UV-vis spectroscopy [23]. From the former titration a μ-oxo-dimerization constant of $K_D = 2.0 \times 10^{-8}$ M was found with an apparent dimerization pH of 6.3 [24].

In Figure 6 (left) the absorption at 394 nm is plotted versus pH for the titration in the presence of **2**. Obviously, the apparent dimerization pH of Fe^{III}TsPP **8** was not affected by the presence of β-cyclodextrin tetramer **2**, indicating that μ-oxo-dimer formation is not hindered by complexation to **2**.

The data for Figure 6 (left) fitted accurately to a model assuming 1 : 1 stoichiometry for the **2**·**9** complex. The formation of the **2**·$\mathbf{9}_2$ complex is not included in this model, since its concentration is negligibly small at the concentrations of host and guest applied in the UV-vis titration. The model encompasses the following equilibria:

Binding of monomeric guest (**8**):

$$\mathbf{2} + \mathbf{8} \rightleftarrows \mathbf{2}\cdot\mathbf{8}, \tag{1}$$

$$\mathbf{2}\cdot\mathbf{8} + \mathbf{8} \rightleftarrows \mathbf{2}\cdot\mathbf{8}_2. \tag{2}$$

Dimerization of the guest into the μ-oxo-dimer (**9**):

$$\mathbf{8} + \mathbf{8} \rightleftarrows \mathbf{9} + 2\mathrm{H}^+. \tag{3}$$

Binding of μ-oxo-dimer **9**:

$$\mathbf{2} + \mathbf{9} \rightleftarrows \mathbf{2}\cdot\mathbf{9}. \tag{4}$$

The titration data were fitted varying the binding constants of **8** and **9** with **2**, and the set of contributions to the observed absorption while using the μ-oxo-dimerization constant K_D as a fixed value. The binding sites occupied in the case of the **2**·$\mathbf{8}_2$ complex were treated as being independent, implying that $K_1 = 8K_2$. A previously described

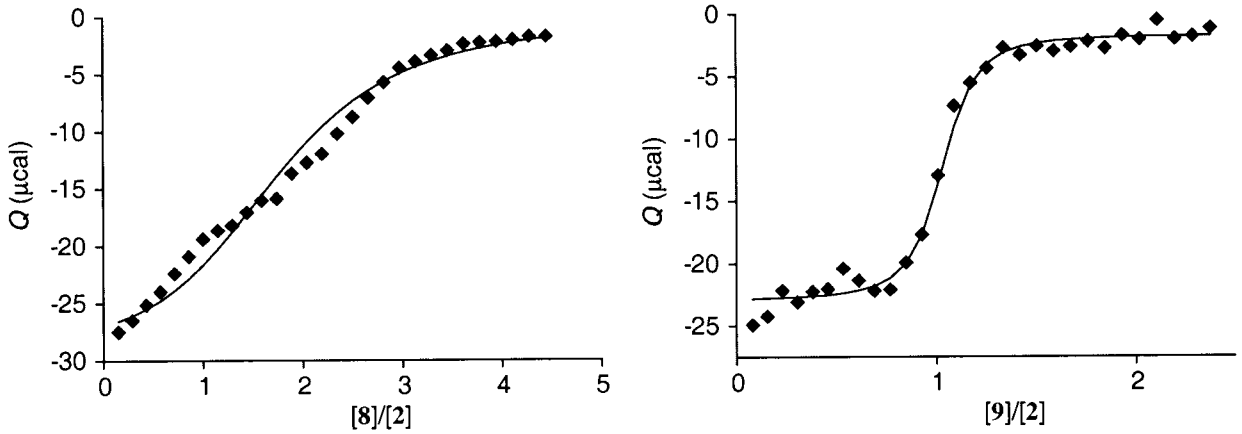

Figure 5. Heat evolved per injection as a function of the ratios [**8**]/[**2**] (left) and [**9**]/[**2**] (right) as observed for the microcalorimetric titrations of monomeric Fe^{III}TsPP **8** and μ-oxo-dimer **9** to β-cyclodextrin tetramer **2**. Lines: fit to a 1 : 2 binding model.

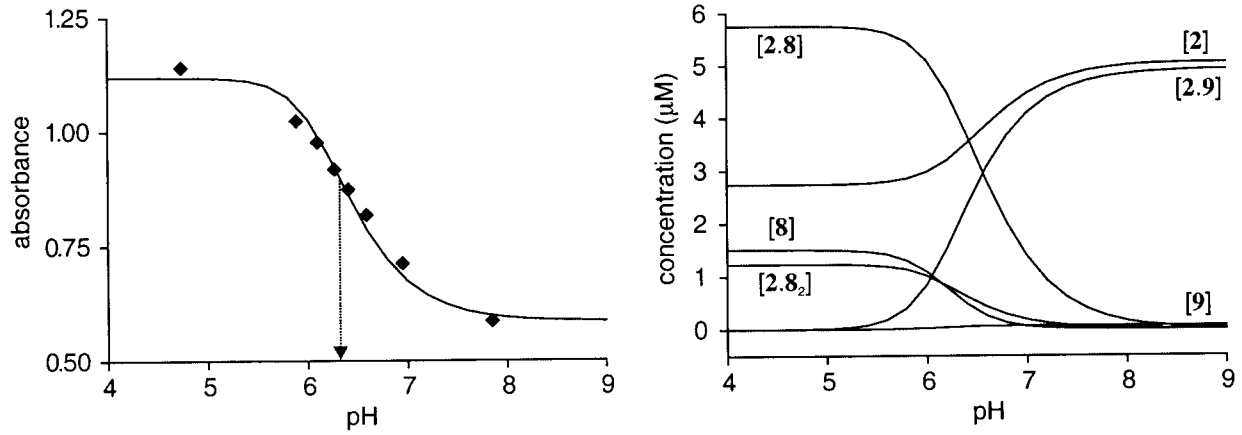

Figure 6. Absorbance at 394 nm as a function of pH of a solution containing 10 μM Fe^{III}TsPP in the presence of 10 μM β-cyclodextrin tetramer **2** (left). The arrow indicates the apparent dimerization pH. The solid line represents the fit to a 1 : 1 binding model. Right: The concentrations of all species as a function of pH for the pH titration of Fe^{III}TsPP **8** in the presence of β-cyclodextrin tetramer **2**.

spreadsheet methodology employing a least squares minimization routine was used for fitting the UV-vis data [25]. Least squares fitting revealed that $A\mathbf{8} \approx A_{\mathbf{2}\cdot\mathbf{8}}$, $A_{\mathbf{2}\cdot\mathbf{8}_2} \approx 2A_{\mathbf{8}}$, and $A_{\mathbf{9}} \approx A_{\mathbf{2}\cdot\mathbf{9}}$, meaning that the molar extinction coefficients of the monoporphyrin and the μ-oxo-dimer are not significantly affected by complexation to the β-cyclodextin tetramer.

The results listed in Table 2 are in good agreement with the data obtained using microcalorimetry listed in Table 1. The species distribution (Figure 6, right) for the pH range of the titration nicely shows that above pH 8 virtually all porphyrin is dimerized to **9** and complexed to β-cyclodextrin tetramer **2**, whereas at low pH the concentration of free Fe^{III}TsPP **8** is relatively high due to weaker complexation.

These studies show that complexation of TsPP-based guests by calix[4]arene-based β-cyclodextrin dimer **1** and tetramer **2** is enhanced as compared to heptakis(2-*O*-methyl)-β-cyclodextrin **6** owing to multiple host–guest interactions. Still, binding strength is raised by only a factor 10 to 20. TsPP **7** and its iron(III) complex **8** are too small for the simultaneous binding of more than two β-cyclodextrins. The strongest binding guest is μ-oxo-dimer **9** although the two porphyrin platforms of **9** are probably too close together for four β-cyclodextrins to bind.

Table 2. Results obtained from the pH titration of Fe^{III}TsPP in the presence of β-cyclodextrin tetramer **2** using UV-vis spectroscopy

Guest	Stoichiometry (host : guest)	K (M^{-1})
8	1 : 1	1.7×10^6
	1 : 2	2.1×10^5
9	1 : 1	1.4×10^7

Since cyclodextrins are bulky molecules, more space around the templated guest sites is required for simultaneous complexation of all four host sites of β-cyclodextrin tetramer **2** without steric hindrance. This is achieved by extension of the porphyrin platform, rather than increasing the number of sites by μ-oxo-dimer formation. *p-Tert*-butylbenzyl-functionalized pyridylporphyrins **10** and **11** (Figure 7) are examples of such extended porphyrins. The *p-tert*-butylbenzyl moiety is known to be strongly complexed by β-cyclodextrin owing to a good match between

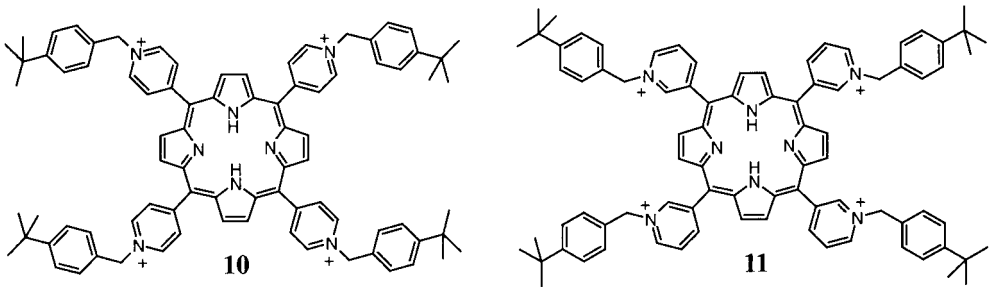

Figure 7. *p-Tert*-butylbenzyl-functionalized *p*- and *m*-pyridylporphyrins (counterions are omitted).

the guest's shape and the dimensions of the β-cyclodextrin cavity.

p-Tert-butylbenzyl-functionalized pyridylporphyrins **10** and **11** were synthesized by reaction of the corresponding tetrapyridylporphyrin precursors with α-bromo-*p-tert*-butyltoluene for 10 h at 80 °C in DMF [15]. The products were purified by precipitation from water as the PF_6 salts using NH_4PF_6. The water-soluble tetrachloride salts of **10** and **11** were obtained by ion exchange chromatography using acetonitrile/water (1 : 1) as the eluent.

In order to determine whether all four binding sites of **10** and **11** are simultaneously accessible, the binding of these guests to native β-cyclodextrin and heptakis(2-*O*-methyl)-β-cyclodextrin **6** was studied using microcalorimetry. Except for the titration of *m*-pyridylporphyrin **11** with **6** the inflection points of the heat profiles indicate simultaneous binding of three cyclodextrins to a porphyrin. On the other hand, CPK models suggest that if it is sterically possible to bind three β-cyclodextrins to **10**, a fourth host can be accommodated as well. For this reason the data were fitted to a 4 : 1 binding model, although a 3 : 1 model gave equally accurate fits.

For the titrations of β-cyclodextrin and heptakis(2-*O*-methyl)-β-cyclodextrin **6** to *p*-pyridylporphyrin **10** the stepwise association constants were all related to K_1 via statistical factors. Furthermore, it was assumed that $\Delta H_1^0 = \Delta H_2^0$ and $\Delta H_3^0 = \Delta H_4^0$. Only K_1, ΔH_1^0, and ΔH_3^0 were used as independently varied fitting parameters. The data for the binding of heptakis(2-*O*-methyl)-β-cyclodextrin **6** to *m*-pyridylporphyrin **11** could only be fitted when also K_3, K_4, ΔH_2^0, and ΔH_4^0 were independently varied. For all titrations, less favorable values for ΔH_3^0 (and ΔH_4^0) compared to ΔH_1^0 (and ΔH_2^0) were obtained while for the binding of **6** to **11** K_3 and K_4 were also decreased. These observations suggest that despite the large dimensions of pyridylporphyrins **10** and **11** steric hindrance still prohibits optimal binding of the third and fourth host. Table 1 summarizes the values found for K_1 and ΔH_1^0 after least squares fitting to a 4 : 1 binding model. The data show that binding strength and enthalpy are decreased for heptakis(2-*O*-methyl)-β-cyclodextrin **6** as compared to native β-cyclodextrin. This same trend has previously been observed for *p-tert*-butylbenzoate as the guest [26].

The complexation of β-cyclodextrin to *p*-pyridylporphyrin **10** was also studied using ^{1}H NMR spectroscopy monitoring the chemical shifts of guest **10** as a function of the β-cyclodextrin/**10** ratio. The results from this titration indicate that at least three cyclodextrins bind to **10** with $K_1 = 2.9 \times 10^4$ M^{-1} (4 : 1 model), which is in agreement with microcalorimetry.

The complexation of calix[4]arene-based β-cyclodextrin dimer **1** with *p*-pyridylporphyrin **10** was studied using microcalorimetry. Figure 8 (left) represents the resulting titration curve. The binding stoichiometry is 2 : 1 (host : guest), as expressed by the inflection point. Table 1 lists the results obtained from the fit of the titration data. The datapoints obtained from the titration of **1** to **10** only gave an accurate fit to a 2 : 1 model assuming non-independent binding sites. The data were fitted using K_1, K_2, ΔH_1^0, and ΔH_2^0 as separately varied parameters.

The error is relatively low for all fitting parameters (20% and 5% for K and ΔH^0, respectively), except for K_1. Accurate fits of the data for *p*-pyridylporphyrin **10** were obtained with values for K_1 in the range 2×10^7–2×10^8 M^{-1}. The complexation of the first β-cyclodextrin dimer **1** to **10** is quite strong and gives rise to an enthalpy change which is almost twice as large as the binding enthalpy observed for the occupation of one *p-tert*-butylbenzyl binding site by a single species of heptakis(2-*O*-methyl)-β-cyclodextrin **6** (−2.5 kcal/mol, see above). Furthermore, K_1 is roughly 20 times the square of the intrinsic binding constant K_i for the **6**·**10** complexes (4.6×10^6 M^{-2}). These observations indicate that in the 1 : 1 complex both β-cyclodextrins of **1** are involved in efficient cooperative binding. The binding of the second dimer to *p*-pyridylporphyrin **10** is enthalpically less favorable ($\Delta H_2^0 < \Delta H_1^0$). Still, regarding the relatively high value of K_2, it is assumed that both β-cyclodextrins of the second host are complexed to both the remaining *p-tert*-butylbenzyl sites. This may occur in a more entropically determined fashion in which the cyclodextrin cavities are less tightly bound than the one host in the 1 : 1 complex. Indeed, $T\Delta S_2^0$ is favorable and approximately equal to $T\Delta S_1^0$.

The binding behavior of β-cyclodextrin dimer **1** to *m*-pyridylporphyrin **11** appears to be more complicated. If **11** is titrated with **1** up to four equivalents, an *endothermic* residual heat effect seems to remain upon dilution of the host (Figure 8, right). However, the residual effect for this titration was proven to be exothermic after all by titrating to a much higher host/guest ratio. After an endothermic value between host : guest ratios of 3 and 6, the pulses became exothermic again near the end of the titration, purely repres-

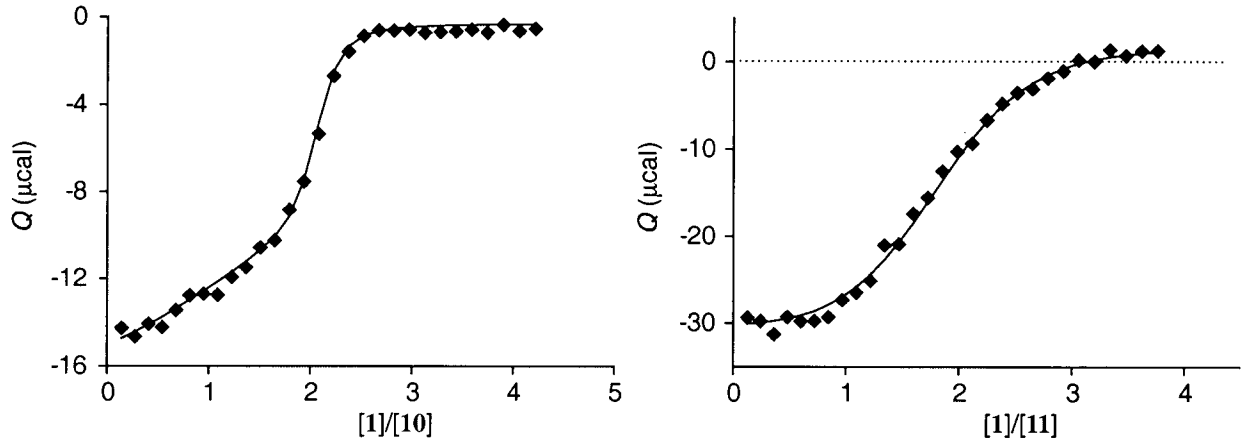

Figure 8. Heat evolved per injection as a function of the ratios [**1**]/[**10**] (left) and [**1**]/[**11**] (right) as observed for the microcalorimetric titrations of β-cyclodextrin dimer **1** to **10** and **11**. Lines: fit to a 2 : 1 binding model (left) and a 4 : 1 binding model (right).

enting the dilution heat. An endothermic complexation heat at $3 < [\mathbf{1}]/[\mathbf{11}] < 6$ can only be accounted for if it is assumed that at high host concentrations a small fraction of the 2 : 1 complex rearranges into 3 : 1 and 4 : 1 complexes in which two hosts only bind via one β-cyclodextrin. Although the data obtained from the titrations of *m*-pyridylporphyrin **11** with β-cyclodextrin dimer **1** were fitted simultaneously to a model assuming non-equivalent binding sites, the results indicate that for the first two binding events the sites can roughly be considered equivalent ($K_1 \approx 12K_2$ and $\Delta H_1^0 \approx \Delta H_2^0$, see Table 1). A statistical factor of 12 between K_1 and K_2 is expected when both opposite and adjacent guest sites are accessible for binding to a dimer, which is a reasonable assumption based on CPK modeling.

Binding enhancement owing to multiple, templated β-cyclodextrins and *p-tert*-butylbenzyl guest sites was most convincingly demonstrated for the 1 : 1 complex of *p*-pyridylporphyrin **10** with β-cyclodextrin tetramer **2** (Figure 9, left). The titration curve has a sharp inflection point at a 1 : 1 host : guest ratio, indicating the formation of a very strong complex. The second inflection point, at a guest : host ratio of about 0.5, indicates the formation of a 2 : 1 (host : guest) complex at relatively high host concentrations.

The data points could only be fitted accurately to a 2 : 1 binding model assuming non-equivalent binding sites. The results are listed in Table 1. The values for K_1 ($5 \times 10^9\ M^{-1}$) and ΔH_1^0 (3.1 times the binding enthalpy for the **6**·**10** complex) suggest that at least three β-cyclodextrins of tetramer **2** are involved in binding to *p*-pyridylporphyrin **10** in the 1 : 1 complex. The value for K_1 is the highest reported to date for cyclodextrin–porphyrin interactions. However, its accuracy is relatively low: the data fit accurately for $K_1 = 2 \times 10^9$–$9 \times 10^9\ M^{-1}$. In contrast to K_1, the error in the other fitting parameters is low (20% for K_2 and 5% for ΔH_1^0 and ΔH_2^0).

The large difference between K_1 and K_2 (roughly a factor 1000) indicates that the complexation of the second β-cyclodextrin tetramer **2** to *p*-pyridylporphyrin **10** is disfavored. Indeed, assuming that three or four β-cyclodextrins of the first host are involved in binding in the 1 : 1 complex, one or two cavities have to decomplex for the second tetramer to bind. The enthalpy values suggest that in the 2 : 1 complex all four binding sites of *p*-pyridylporphyrin **10** are complexed by a β-cyclodextrin host site of **2**.

Figure 9 (right) shows the curve obtained from the titration of *m*-pyridylporphyrin **11** to β-cyclodextrin tetramer **2**. As in the case of the complexation of **11** to β-cyclodextrin dimer **1**, the situation seems to be more complicated than with *p*-pyridylporphyrin **10** as the guest. Due to three inflection points (at [**11**]/[**2**] ratios of 0.5, 0.8, and 1.5) the data could not be fitted to models assuming exclusively 1 : 1 and 1 : 2 or 1 : 1 and 2 : 1 binding stoichiometries. A satisfying fit was obtained only using a model assuming the formation of 1 : 1, 1 : 2, and 2 : 1 complexes of *m*-pyridylporphyrin **11** and β-cyclodextrin tetramer **2**. However, higher order complexes cannot be excluded and the association constants varied a lot without affecting the accuracy of the fit.

In general, despite their structural similarity *p-tert*-butylbenzyl-appended pyridyl porphyrins **10** and **11** showed quite different complexation behavior to the calix[4]arene-based β-cyclodextrin dimer **1** and tetramer **2** and heptakis(2-*O*-methyl)-β-cyclodextrin **6**. In fact, the results obtained with **10** were often more easy to explain than the data obtained from studies involving **11** as a guest. A marked difference between **10** and **11** is the fact that rotation around the C_{meso}–C_{pyr} and N_{pyr}–C_{benz} bonds gives rise to much more conformational variation in the case of **11**. CPK modeling even showed the possibility of placing one or more *p-tert*-butyl groups above the plane of the porphyrin, which is not possible in the case of **10**.

Conclusions

If the guest has multiple binding sites for β-cyclodextrin and enough space per site, complexation by a host which has multiple cyclodextrin sites results in very strong complexes. The present study as well as several previous investigations [9–11] proved the suitability of porphyrin-templated guests for binding to β-cyclodextrin dimers and tetramers. Cooperative binding is achieved by creating more space per guest

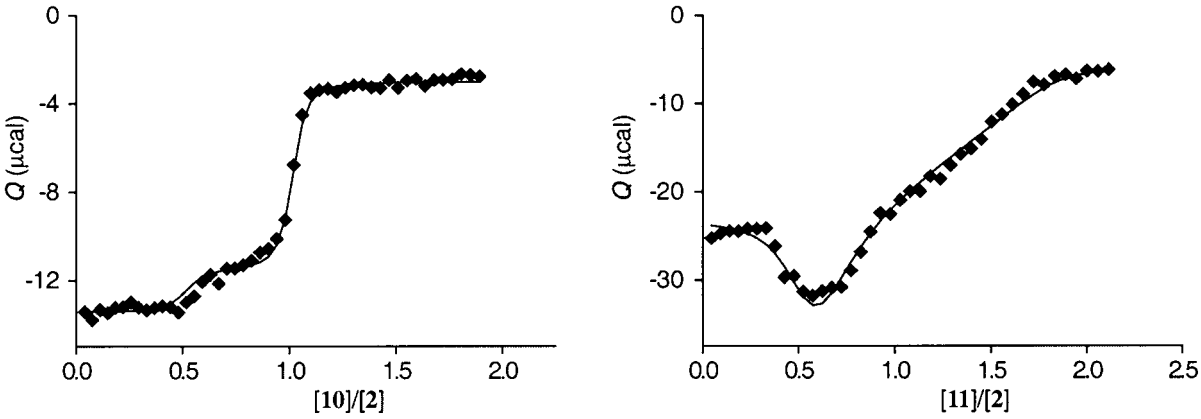

Figure 9. Heat evolved per injection as a function of the ratios [**10**]/[**2**] (left) and [**11**]/[**2**] (right) as observed for the microcalorimetric titrations of **10** and **11** to β-cyclodextrin tetramer **2**. Lines: fit to a 2 : 1 binding model (left) and a model assuming both 1 : 2 and 2 : 1 stoichiometry (right).

site via extension of the porphyrin platform, rather than by combining two metallated porphyrins into a μ-oxo-dimer, which only increases the number of guest sites. The 1 : 1 complex between guest **10** and tetramer **2** ($K = 5 \times 10^9$ M^{-1}) is the strongest reported for cyclodextrin–porphyrin interactions. The systems described here may find application in aqueous catalysis. Large host molecules, such as **2**, having multiple cyclodextrin sites, may be able to bring a catalytically active species, such as a metallated porphyrin, and organic substrates in close proximity via non-covalent binding, which may lead to enhancement of reaction rates.

References

1. L. Stryer: *Biochemistry* 3rd ed., W.H. Freeman and Company: New York (1988).
2. J.P. Collman and L. Fu: *Acc. Chem. Res.* **32**, 455 (1999).
3. K. Tomizaki, T. Murata, K. Kaneko, A. Miike, and N. Nishino: *J. Chem. Soc., Perkin Trans. 2* 1067 (2000).
4. S. Hamai and T. Koshiyama: *J. Photochem. Photobiol. A* **127**, 135 (1999).
5. J.M. Ribó, J.-A. Farrera, M.L. Valero, and A. Virgili: *Tetrahedron* **51**, 3705 (1995).
6. D.L. Dick, T.V.S. Rao, D. Sukumaran, and D.S. Lawrence: *J. Am. Chem. Soc.* **114**, 2664 (1992).
7. R. Rubires, J. Crusats, Z. El-Hachemi, T. Jaramillo, M. López, E. Valls, J.-A. Farrera, and J.M. Ribó, *New J. Chem.* 189 (1999).
8. T. Carofiglio, R. Fornasier, V. Lucchini, C. Rosso, and U. Tonellato: *Tetrahedron Lett.* **37**, 8019 (1996).
9. T. Jiang and D.S. Lawrence: *J. Am. Chem. Soc.* **117**, 1857 (1995).
10. F. Venema, A.E. Rowan, and R.J.M. Nolte: *J. Am. Chem. Soc.* **118**, 257 (1996).
11. F. Venema, H.F.M. Nelissen, P. Berthault, N. Birlirakis, A.E. Rowan, M.C. Feiters, and R.J.M. Nolte: *Chem. Eur. J.* **4**, 2237 (1998).
12. T. Jiang, M. Li, and D.S. Lawrence: *J. Org. Chem.* **60**, 7293 (1995).
13. M. Larsen and M. Jørgensen: *J. Org. Chem.* **61**, 6651 (1996).
14. E. van Dienst, B.H.M. Snellink, I. von Piekartz, and M.H.B. Grote Gansey, F. Venema, M.C. Feiters, R.J.M. Nolte, J.F.J. Engbersen, and D.N. Reinhoudt: *J. Org. Chem.* **60**, 6537 (1995).
15. T. Mizutani, T., Horiguchi, H. Koyama, I. Uratani, and H. Ogoshi: *Bull. Chem. Soc. Jpn.* **71**, 413 (1998).
16. C.D. Gutsche: *J. Org. Chem.* **50**, 5795 (1985).
17. C.D. Gutsche and P.A. Reddy: *J. Org. Chem.* **56**, 4783 (1991).
18. P. Linnane, T.D. James, and S. Shinkai: *J. Chem. Soc., Chem. Commun.* 1997 (1995).
19. R.H. Vreekamp: Ph.D. Thesis, University of Twente (1995).
20. S. Mosseri, J.C. Mialocq, B. Perly, and P. Hambright: *J. Phys. Chem.* **95**, 4659 (1991).
21. E.B. Fleischer, J.M. Palmer, T.S. Srivastava, and A. Chatterjee: *J. Am. Chem. Soc.* **93**, 3162 (1971).
22. F. Venema: Ph.D. Thesis, University of Nijmegen (1996).
23. This absorption band shows a redshift (394 $\rightarrow$ 410 nm) upon formation of the μ-oxo-dimer [21].
24. The obtained value for K_D (2.0×10^{-8} M) is in reasonable agreement with Fleischer's value (8.0×10^{-9} M) [21].
25. J. Huskens, H. van Bekkum, and J.A. Peters: *Comp. Chem.* **19**, 409 (1995).
26. Th. Höfler and G. Wenz: *J. Incl. Phenom.* **25**, 81 (1996).